About the exam

Oral exam,
about 12 min. preparation with no documents, 12 min. on the board

Typical questions:

What is the corrugation ?

Explain the principles of tunneling spectroscopy.

Questions related to an image discussed in the lecture

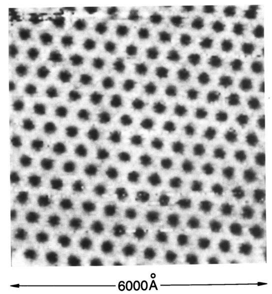

Fig. 4.120. Abrikosov flux lattice produced by 1 T magnetic field in $NbSe_2$ at 1.8 K. The gray scale corresponds to dI/dU (Hess *et al.*, 1989).

Explain how a scanner tube works

Chapter 4
Scanning Tunneling Spectroscopy

4.5: Spin-resolved STM

Spin-resolved STM principle

An electron has a spin.
Spin conserved in tunneling, two independent channels co-exist:

$$\boxed{I_t = I_\uparrow + I_\downarrow}$$

Basis for spin-sensitive STM.
Detect with STM the images of spin up or down electrons.

A practical difficulty is to control the tip magnetization, at its very apex.

Spin-resolved STM: a naive picture

Stoner model: spin up and down shifted by the exchange energy.

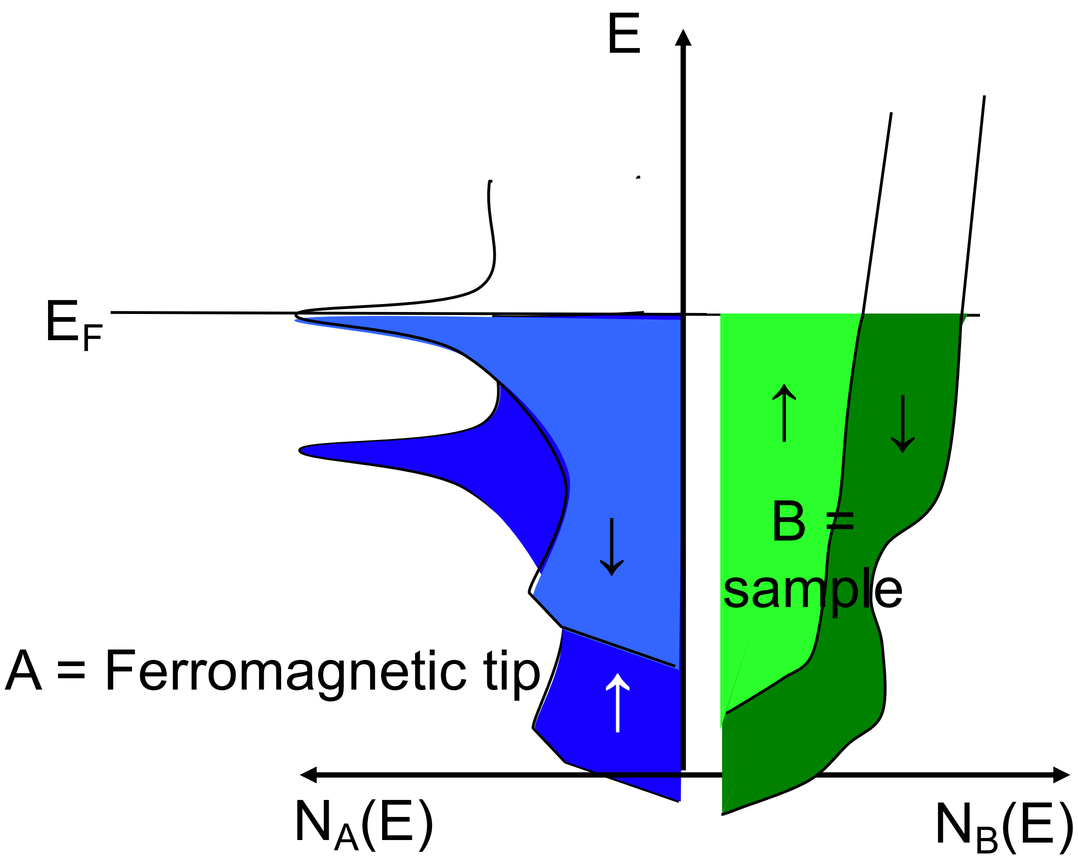

Spin-resolved STM: a naive picture

Stoner model: spin up and down shifted by the exchange energy.

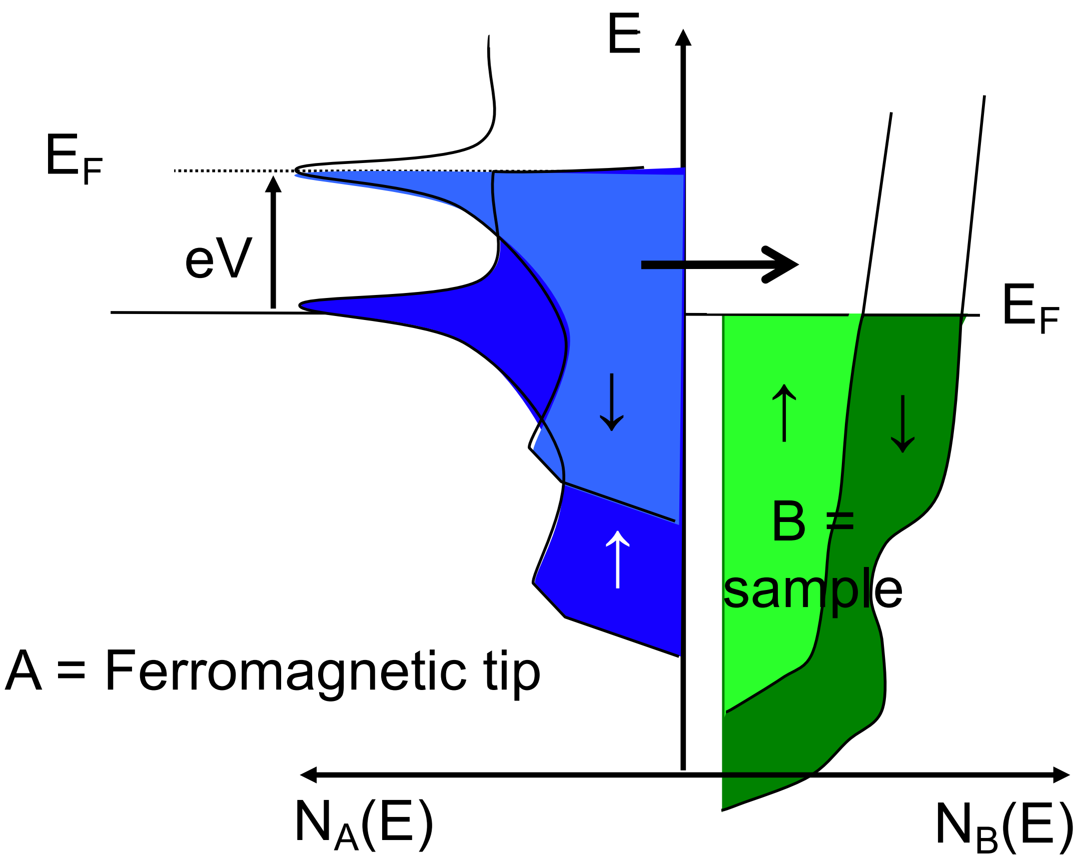

Compare cases of a tip ↑ or ↓.

Here I(V) (hence topography) little sensitive to spin.

Tunneling spectroscopy

Full expression of the tunnel current:

$$\mathrm{I} \propto \int_{-\infty}^{+\infty} \mathrm{N_A(E-eV)N_B(E)[f(E)-f(E-eV)]dE}$$

At zero temperature:

$$\mathrm{I} \propto \int_{\mathrm{E_F}}^{\mathrm{E_F+eV}} \mathrm{N_A(E-eV)N_B(E)dE} = \int_{\mathrm{E_F-eV}}^{\mathrm{E_F}} \mathrm{N_A(E')N_B(E'+eV)dE'}$$

Differential conductance (hyp. N_B does not vary much with E):

$$\frac{\mathrm{dI}}{\mathrm{dV}} \propto \mathrm{N_A(E_F-eV)N_B}$$

Tunneling spectroscopy, with the spin

Differential conductance (hyp. N_B does not vary much with E):

$$\frac{dI}{dV} \propto N_A(E_F - eV)N_B$$

Taking into account the spin, two channels in parallel:

$$\frac{dI}{dV} \propto N_{A\uparrow}(E_F - eV)N_{B\uparrow} + N_{A\downarrow}(E_F - eV)N_{B\downarrow}$$

If the DOS of A at the energy E_F – eV is mainly spin up:

$$\frac{dI}{dV} \sim \frac{dI_\uparrow}{dV} \propto N_{A\uparrow}(E_F - eV)N_{B\uparrow} \propto N_{B\uparrow}$$

Spin-resolved STM: a naive picture

Stoner model: spin up and down shifted by the exchange energy.

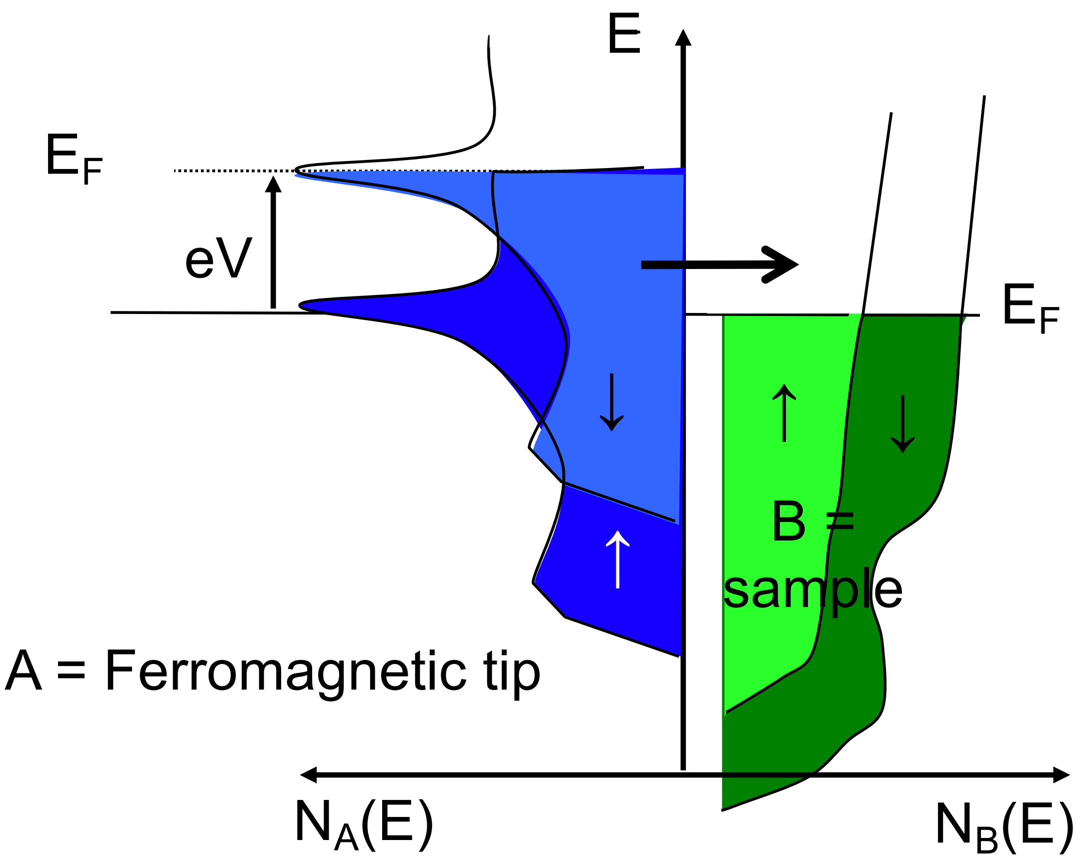

Compare cases of a tip ↑ or ↓.

Here I(V) (hence topography) little sensitive to spin.

At a well-chosen bias, dI/dV can be dominated by a spin population:

$$\frac{dI}{dV} \sim \frac{dI_{\uparrow}}{dV} \propto N_{A\uparrow}(E_F - eV) N_{B\uparrow} \propto N_{B\uparrow}$$

in the present case

(T -> 0)

Magnetic vortices (1)

a.c. bias modulation added to d.c..

Different contrast between topography image (constant current regulation) and dI/dV (magnetic image).

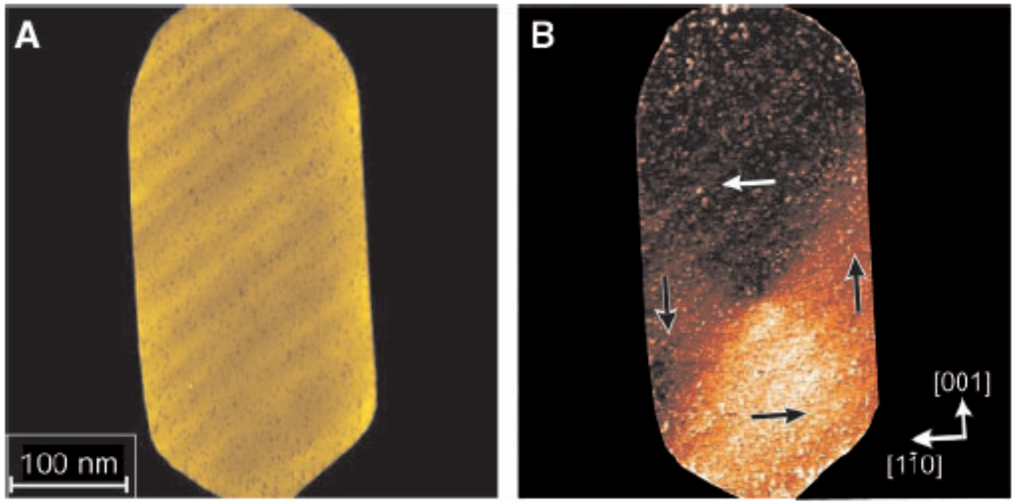

Fig. 2. (**A**) Topography and (**B**) map of the dI/dU signal of a single 8-nm-high Fe island recorded with a Cr-coated W tip. The vortex domain pattern can be recognized in (B). Arrows illustrate the orientation of the domains. Because the sign of the spin polarization and the magnetization of the tip is unknown, the sense of vortex rotation could also be reversed. The measurement parameters were I = 0.5 nA and U_0 = +100 mV. The crystallographic orientations were determined by low-energy electron diffraction.

First direct observation of a magnetic vortex.

Here tip is magnetized in-plane.

Has nothing to do with a superconductor’s vortex!

A. Wachowiak, R. Wiesendanger et al, Science 298, 577 (2002).

Magnetic vortices (2)

Tip with an in-plane or out-of-plane magnetization:

gives access to the two components of the sample magnetization.

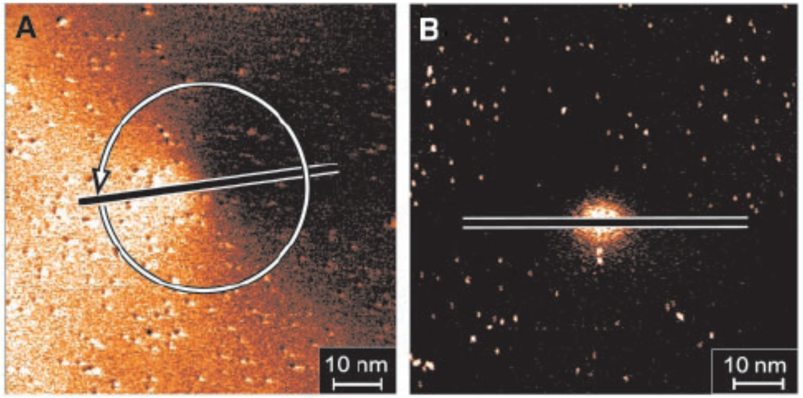

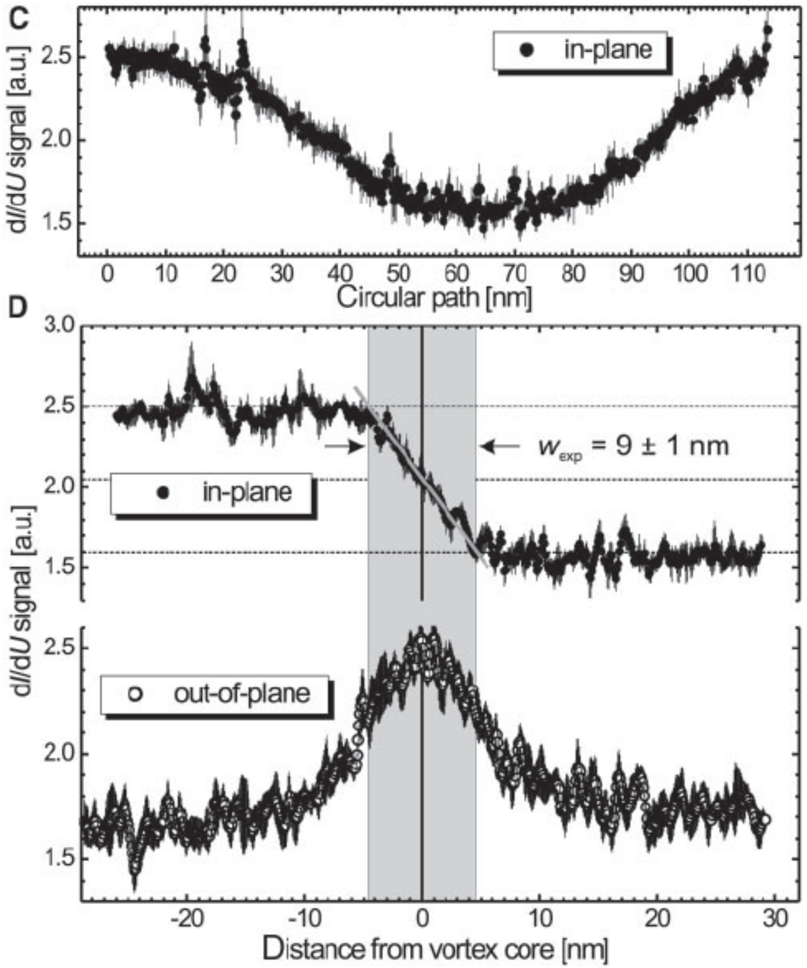

Fig. 3. Magnetic dI/dU maps as measured with an **(A)** in-plane and an **(B)** out-of-plane sensitive Cr tip. The curling in-plane magnetization around the vortex core is recognizable in (A), and the perpendicular magnetization of the vortex core is visible as a bright area in (B). **(C)** dI/dU signal around the vortex core at a distance of 19 nm [circle in (A)]. **(D)** dI/dU signal along the lines in (A) and (B). The measurement parameters were (A) $I = 0.6$ nA, $U_0 = -300$ mV and (B) $I = 1.0$ nA, $U_0 = -350$ mV.

Magnetic spatial resolution here down to 5 nm, much better than MFM.

Magnetism of a single atom

Magnetic imaging down to the single atom scale.

F. Meier et al. Science 320, 82 (2008).

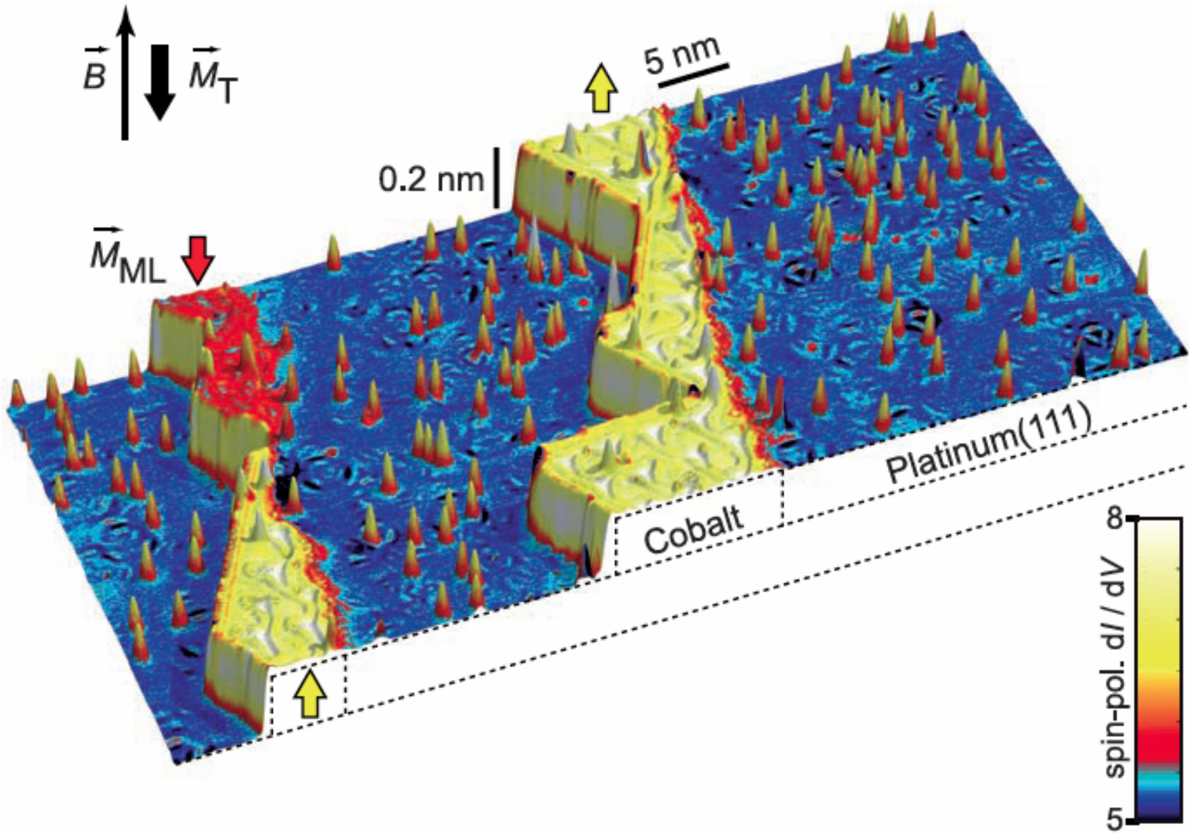

Fig. 1. Overview of the sample of individual Co adatoms on the Pt(111) surface (blue) and Co ML stripes (red and yellow) attached to the step edges (STM topograph colorized with the simultaneously recorded spin-polarized dI/dV map measured with an STM tip magnetized antiparallel to the surface normal). An external $\vec{B}$ can be applied perpendicular to the sample surface in order to change the magnetization of adatoms $\vec{M}_A$, ML stripes $\vec{M}_{ML}$, or tip $\vec{M}_T$. The ML appears red when $\vec{M}_{ML}$ is parallel to $\vec{M}_T$ and yellow when $\vec{M}_{ML}$ is antiparallel to $\vec{M}_T$. (Tunneling parameters are as follows: $I = 0.8$ nA, $V = 0.3$ V, modulation voltage $V_{mod} = 20$ mV, $T = 0.3$ K.)

Revealing magnetic interactions

Single atom magnetization cycles: give access to the local exchange energy.

Fig. 4. Magnetic exchange between adatoms and ML stripe. (**A** to **C**) Magnetization curves measured on the ML (straight lines) and on the three adatoms (dots) A, B, and C visible in the inset topograph of (D). The blue color indicates the down sweep from $B = +1$ T to -1 T (and red, the up sweep from -1 T to $+1$ T) (dI/dV signal on ML inverted for clarity). The vertical arrows indicate the exchange bias field, B_{ex}, which is converted into the exchange energy (using $m = 3.7\mu_B$) for the corresponding magenta points in the plot (D). (Tunneling parameters are as follows: $I = 0.8$ nA, $V = 0.3$ V, $V_{mod} = 20$ mV, $T = 0.3$ K.) (**D**) Dots show measured exchange energy as a function of distance from ML as indicated by the arrow in the inset (about 50° to [11$\bar{2}$]). The black line is the dipolar interaction calculated from the stray field of a 10-nm-wide stripe with saturation magnetization 1.3×10^6 A/m. The red, blue, and green lines are fits to 1D, 2D, and 3D range functions for indirect exchange. Horizontal error bars are due to the roughness of the Co-ML-stripe edge, whereas the vertical ones are due to the uncertainty in B_{ex}.

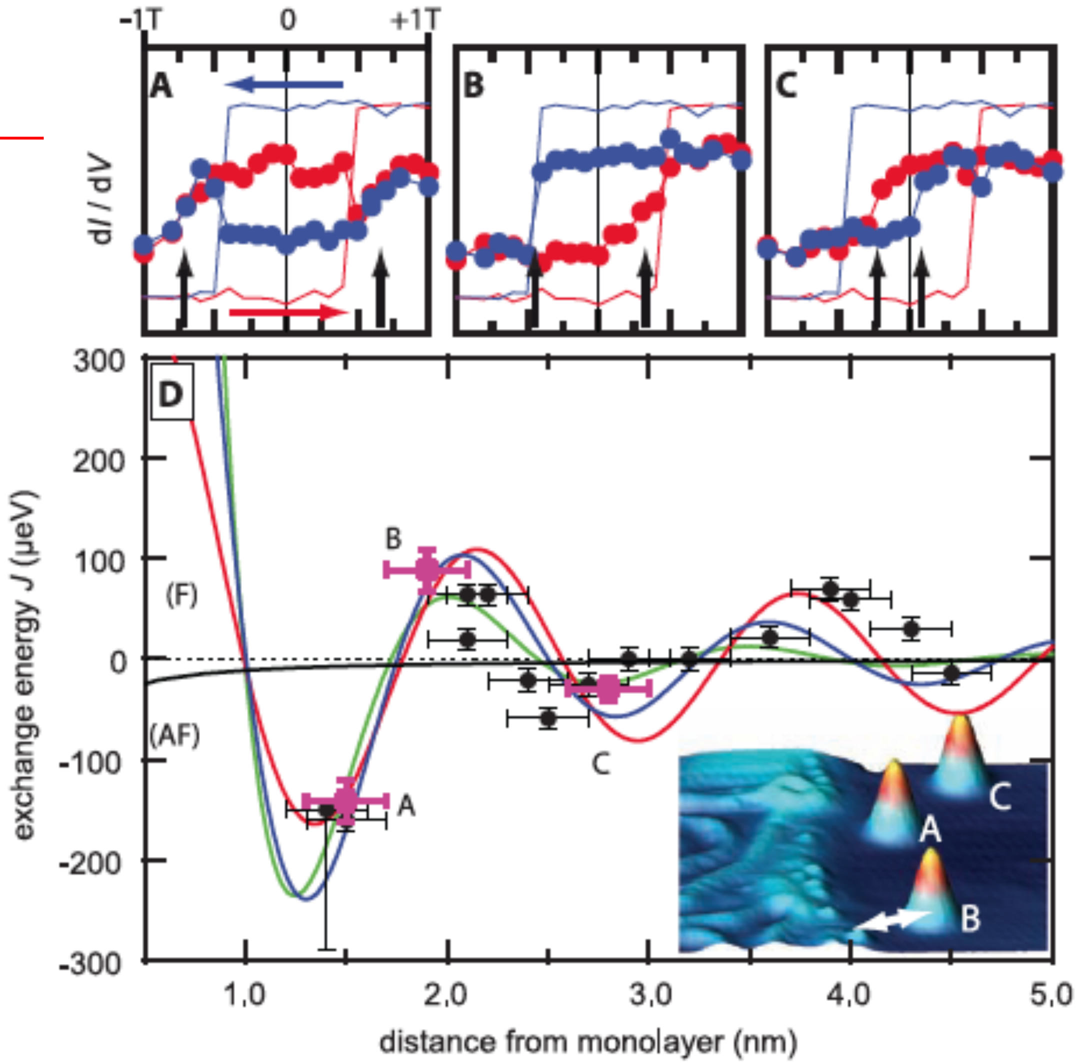

Oscillatory, RKKY-type interactions are revealed.

Chapter 5

Nano-manipulation

Chapter 5
Nano-manipulation

5.1: Surface states

Atom manipulation

For example: clean Ni surface with Xe atoms.

Low temperature (4 K) to freeze atom diffusion.

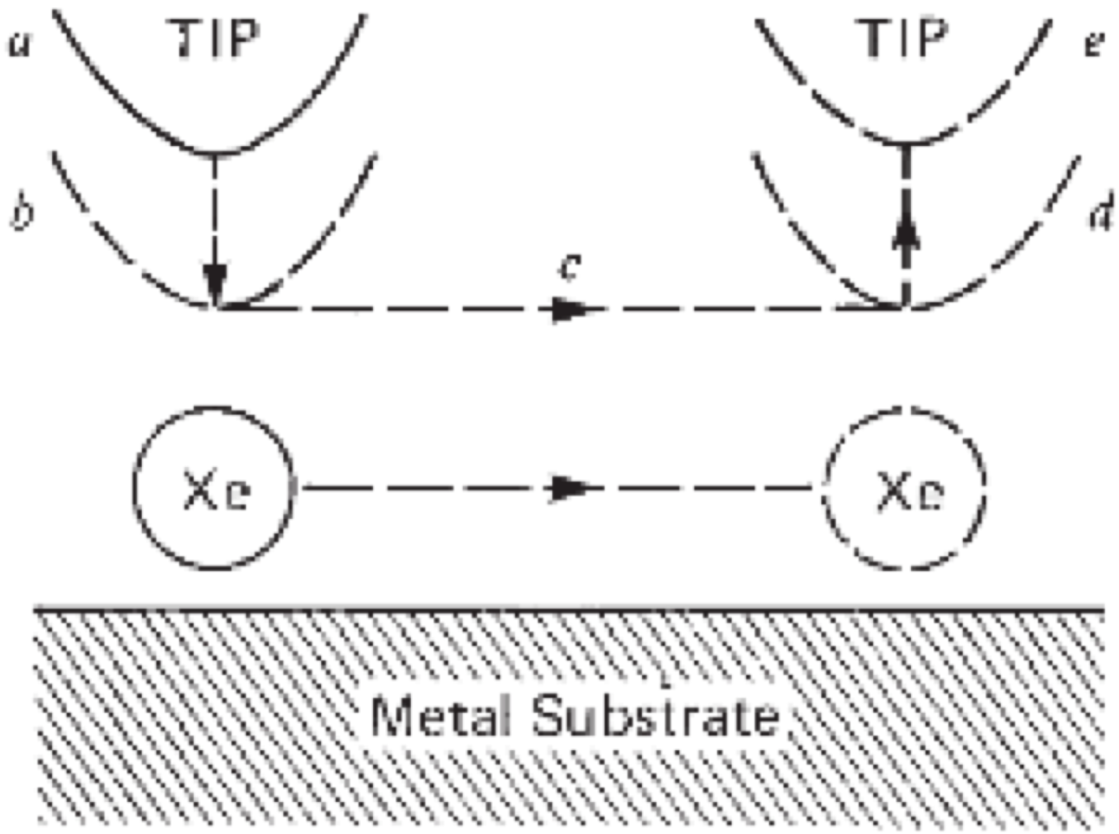

Tunnel image at 10 mV/1 nA,

Atom manipulation possible by increasing current up to 16 nA.

Atom manipulation

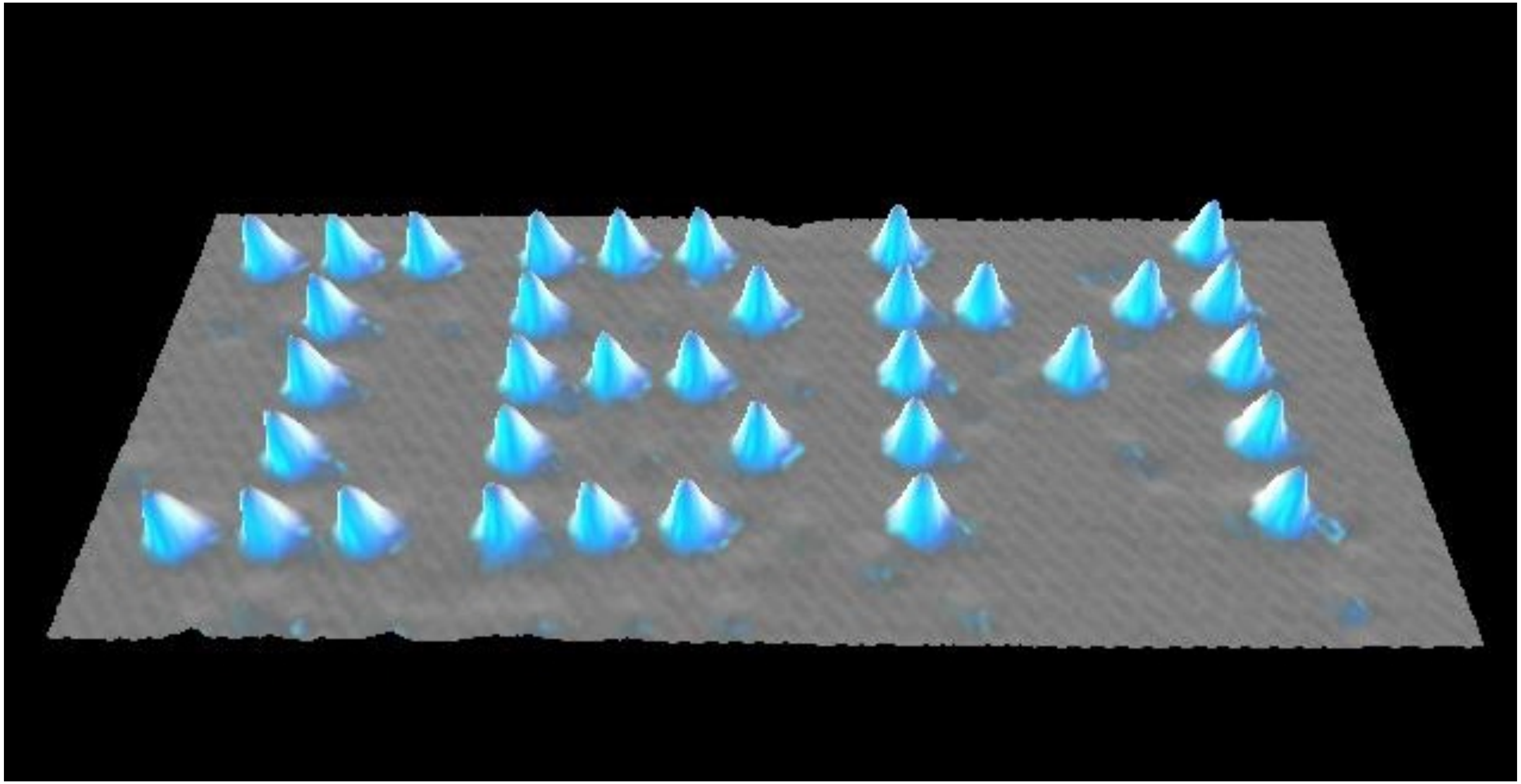

D.M. Eigler and E.K. Schweizer, Nature 344, 524 (1990)

Electronic surface states

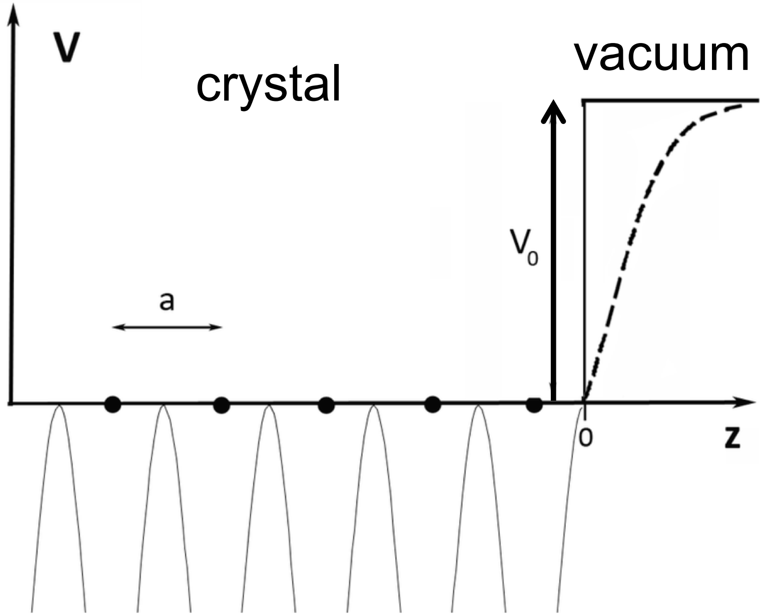

Near a metal surface, e- feel a potential different from the bulk:

In addition to bulk states, surface states appear in E(k) forbidden regions (for bulk states).

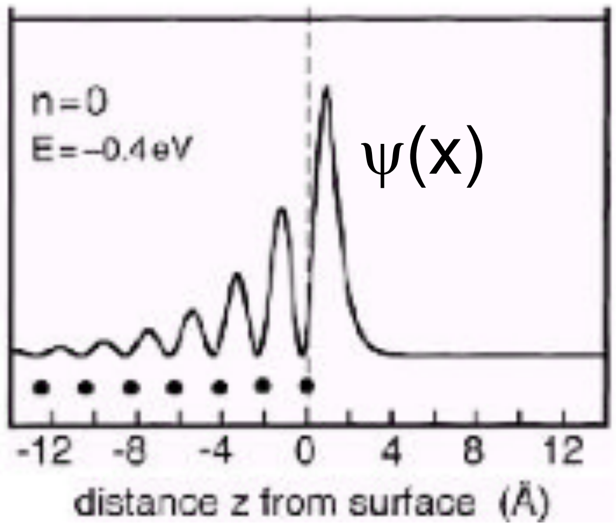

Figures from S. Pons thesis, Grenoble (2000)

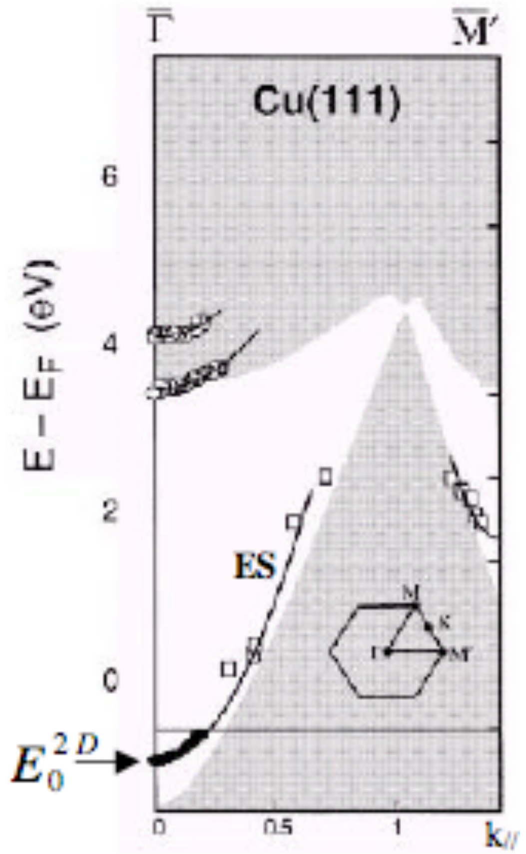

The quantum corral

Co atoms on a Cu surface reflect the surface state wave:

The corral creates a stationary wave of surface states.

In french: “enclos“, not “corail“.

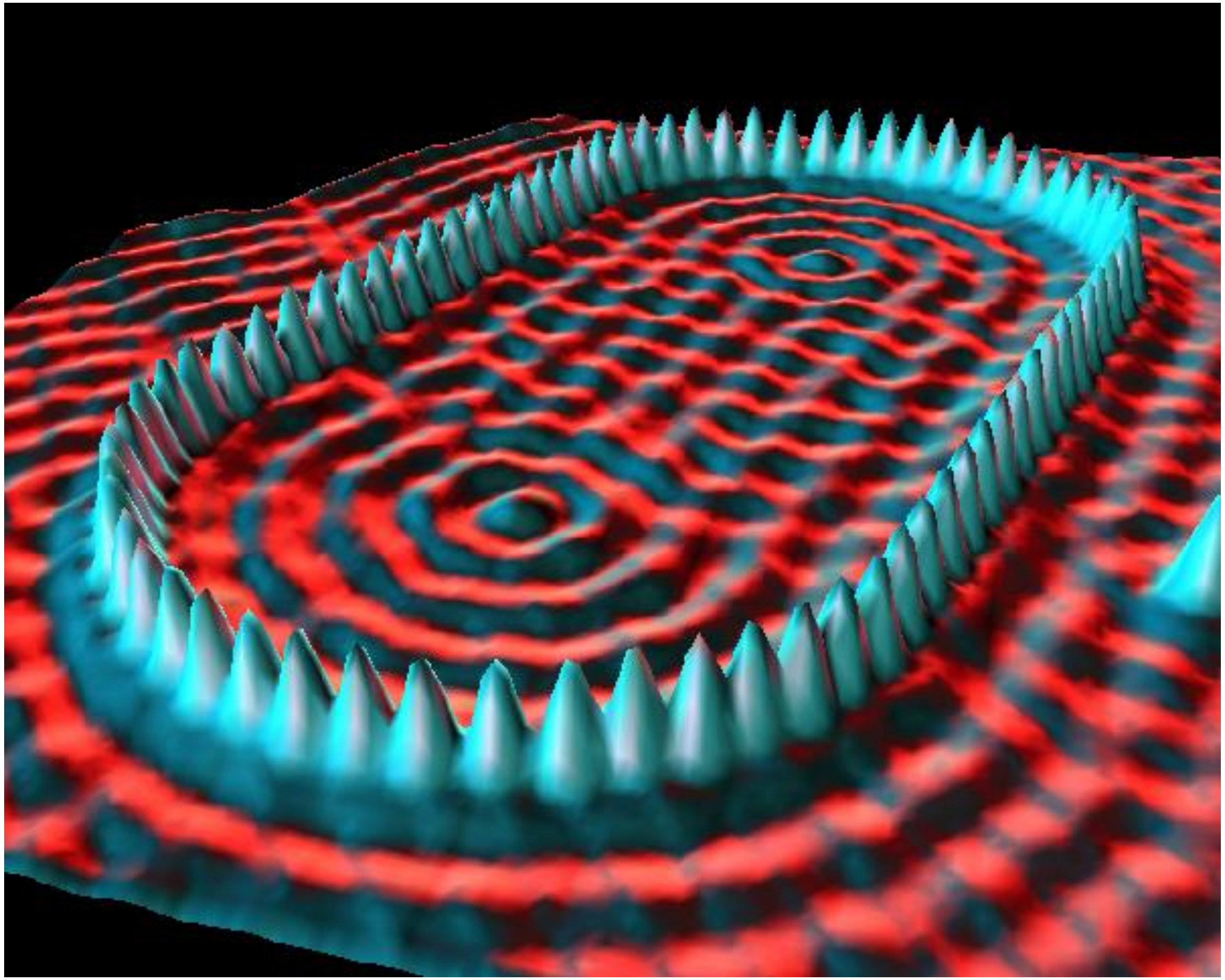

M.F. Crommie, C.P. Lutz and D.M. Eigler, Science 262, 218 (1993), http://www.almaden.ibm.com/vis/stm/gallery.html

The making of

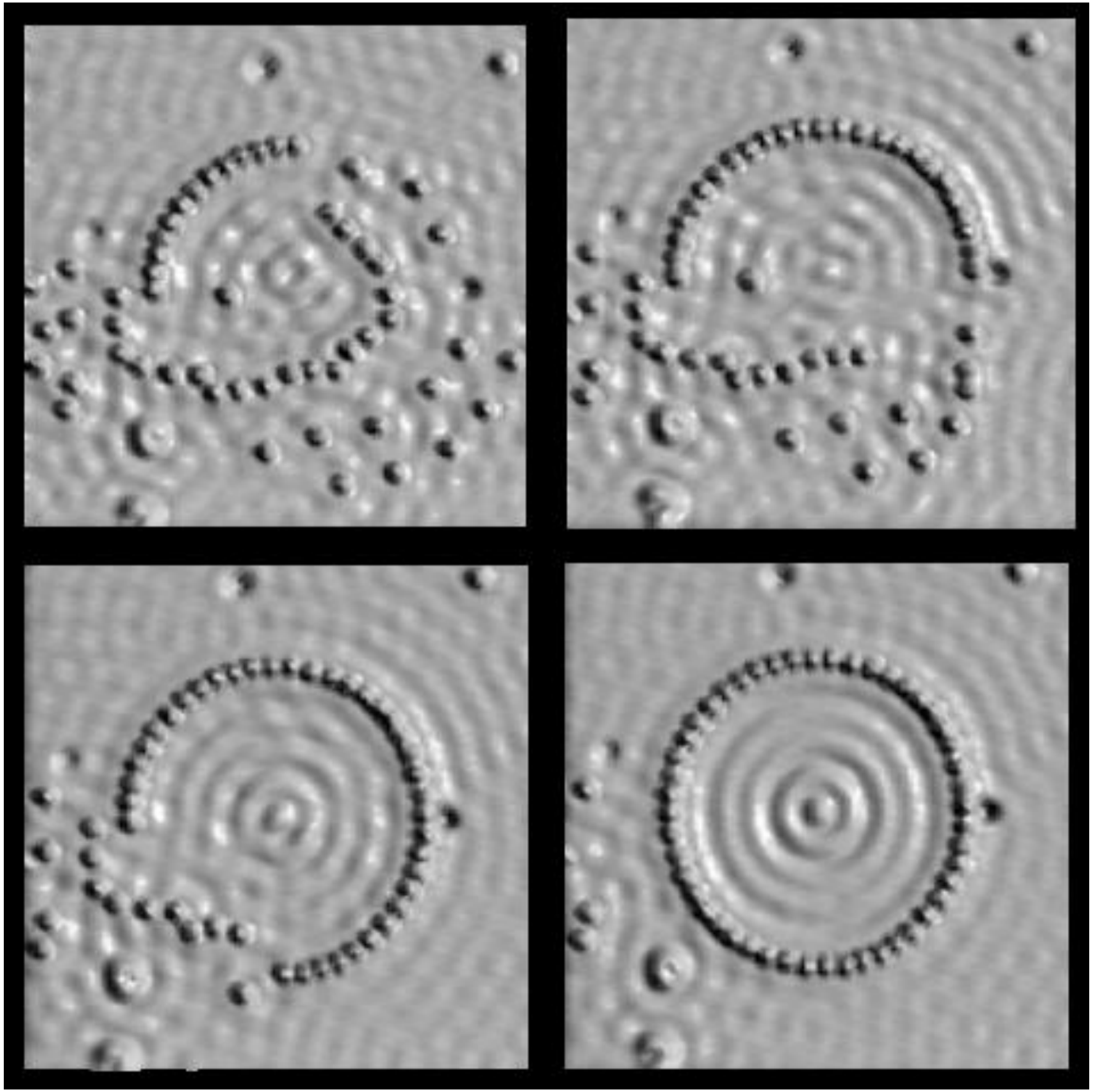

The Kondo effect

Magnetic impurity (Co) in a metal (Cu): Kondo effect

LDOS: destructive interference between transitions into localized and delocalized orbitals near Fermi level.

(b) = topography.
(c) = conductance map with bias close to Kondo anomaly.

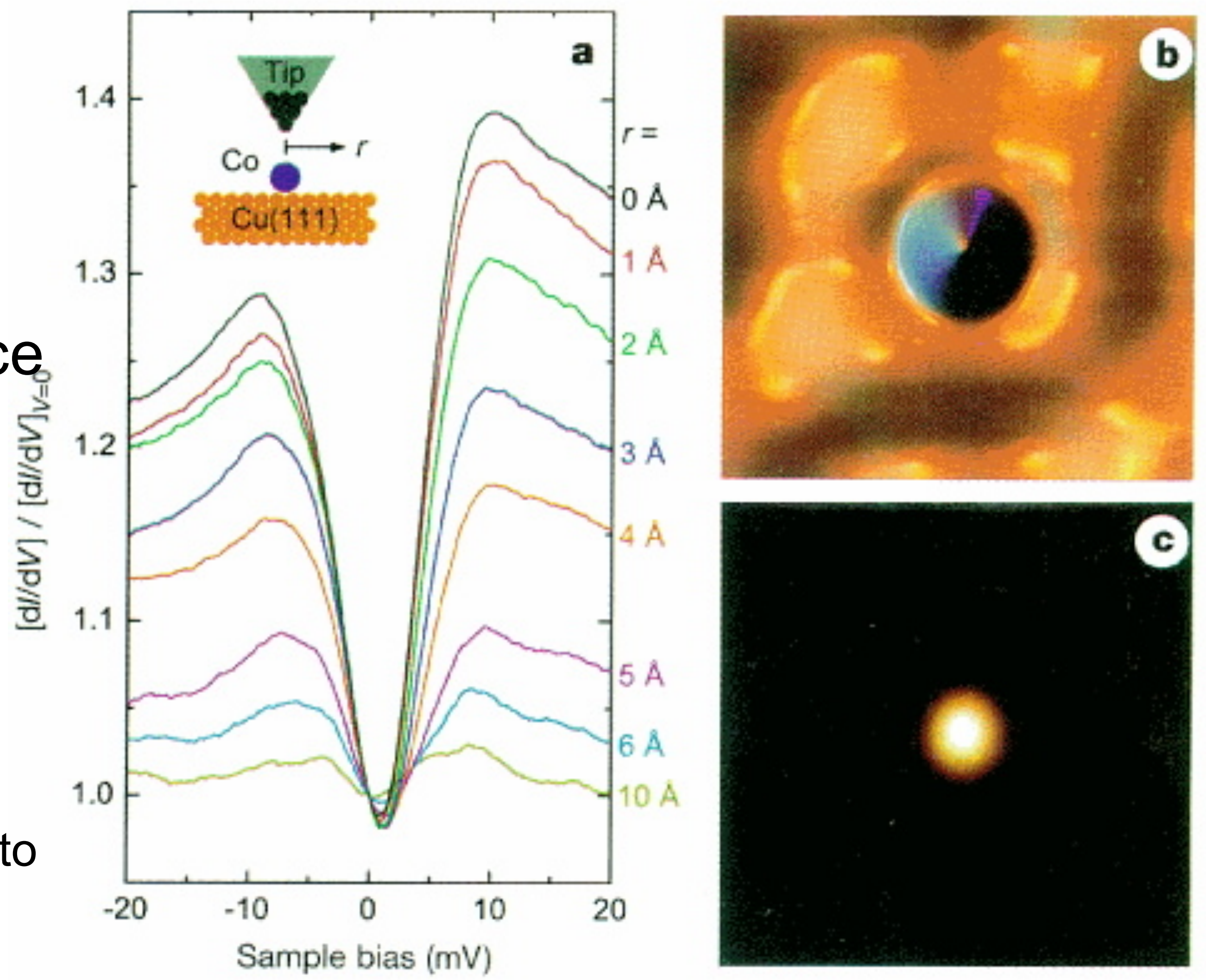

The quantum mirage

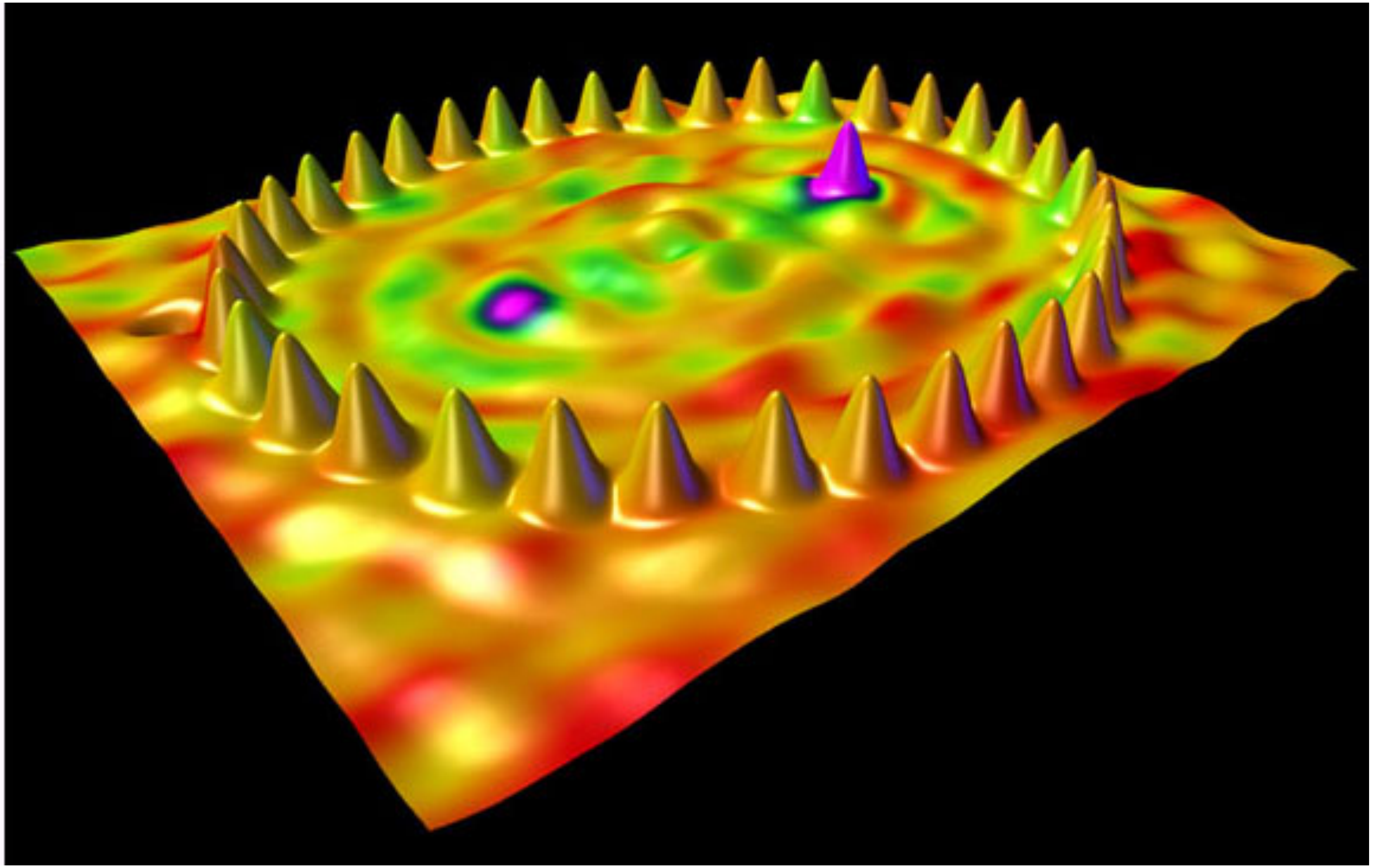

Elliptic corral: electronic waves originating from one focus are converging on the other focus.

H.C. Manoharan, C.P. Lutz and D.M. Eigler, Nature 403, 512 (2000)

Chapter 5
Nano-manipulation

5.2: Nano-oxidation lithography

Local anodization with an AFM (1)

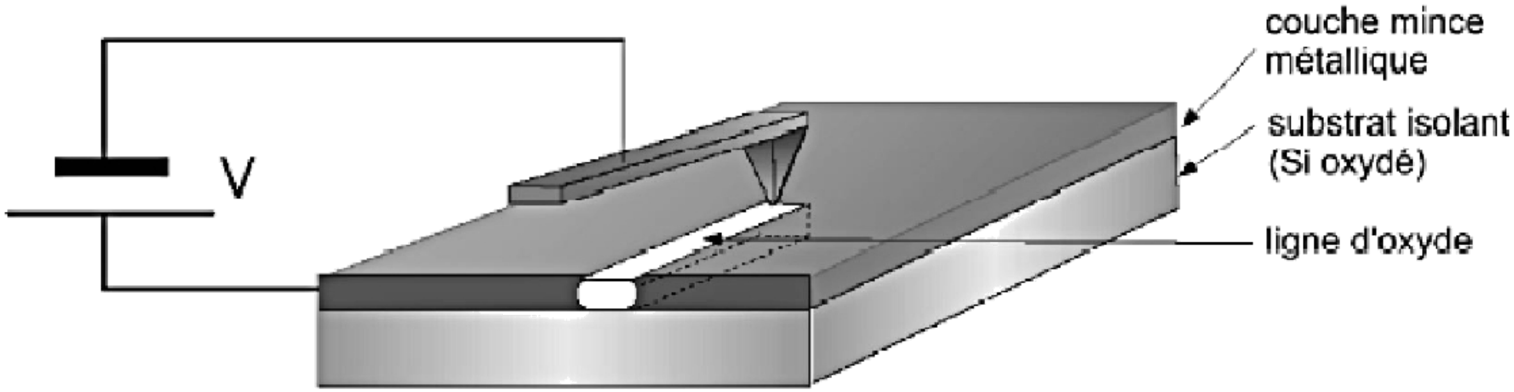

Figure from M. Faucher thesis, Grenoble (2003).

Metallized tip with a voltage bias of about 4 V:
+ Water meniscus below the tip apex =
Local anodization

If the metal layer is thin enough (< 5 nm), the oxyde can go through the whole layer : circuit patterning is possible.

Superconducting Quantum Interference Device (SQUID)

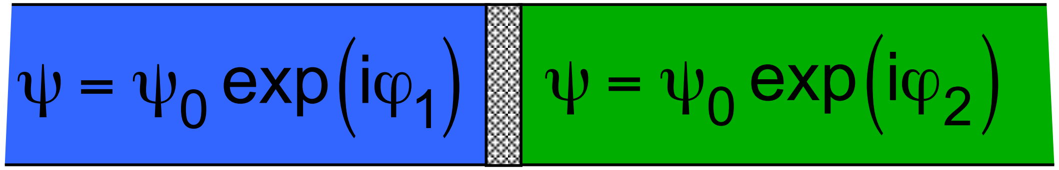

Josephson effect in a tunnel junction between two superconductors:

superconducting tunnel current = $I_S = I_c \sin(\varphi_2 - \varphi_1)$

I_c = critical current,

$\varphi = \varphi_2 - \varphi_1$ = phase difference between the two condensates.

SQUID = two Josephson junctions in parallel.

ϕ = magnetic field flux

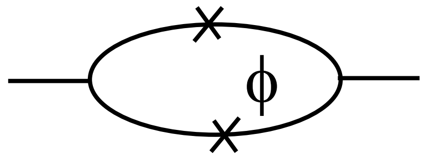

Superconducting Quantum Interference Device (SQUID)

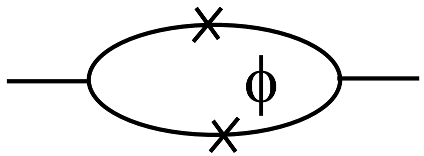

The two supercurrents add coherently.

Flux though the loop adds a potential vector term A.S = $2\pi\Phi/\Phi_0$

If loop self-inductance can be neglected:

$$I_S = I_{c0}\sin\left(\varphi_2 - \varphi_1 - \pi\frac{\phi}{\phi_0}\right) + I_{c0}\sin\left(\varphi_2 - \varphi_1 + \pi\frac{\phi}{\phi_0}\right) = 2I_{c0}\sin(\varphi_2 - \varphi_1)\cos\left(\pi\frac{\phi}{\phi_0}\right)$$

where $\Phi_0 = h/2e$ is the superconducting flux quantum.

Critical current is modulated by the magnetic flux through the loop, even if there is no flux through the two wires. Analogous to Young's slits.

$$I_S = I_c\sin(\varphi_2 - \varphi_1) \quad \text{where} \quad I_c = 2I_{c0}\left|\cos\left(\pi\frac{\phi}{\phi_0}\right)\right|$$

Local anodization with an AFM (2)

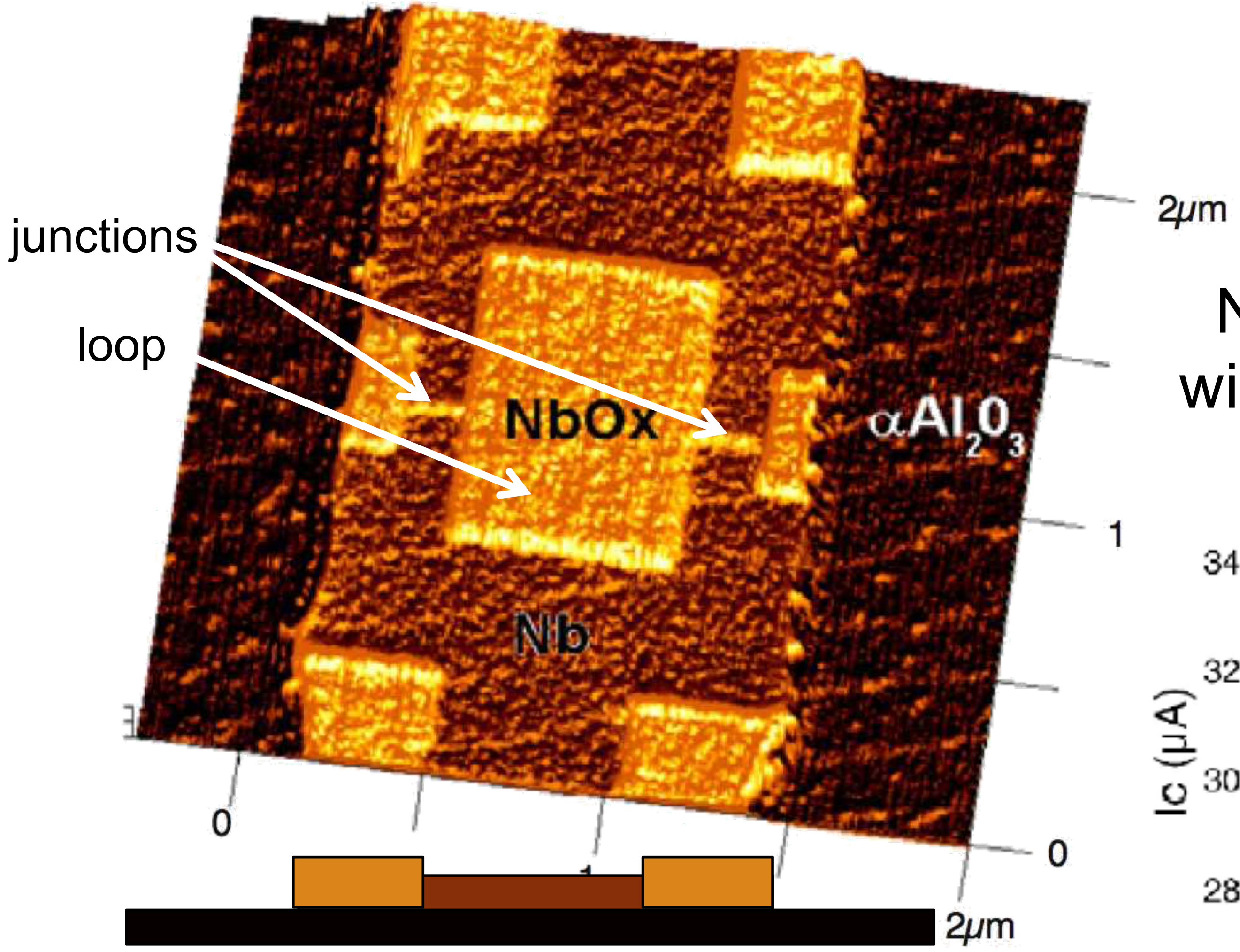

AFM image of a circuit: oxyde appears as thicker.

Nb loop circuit : SQUID effect with a flux quantum periodicity.

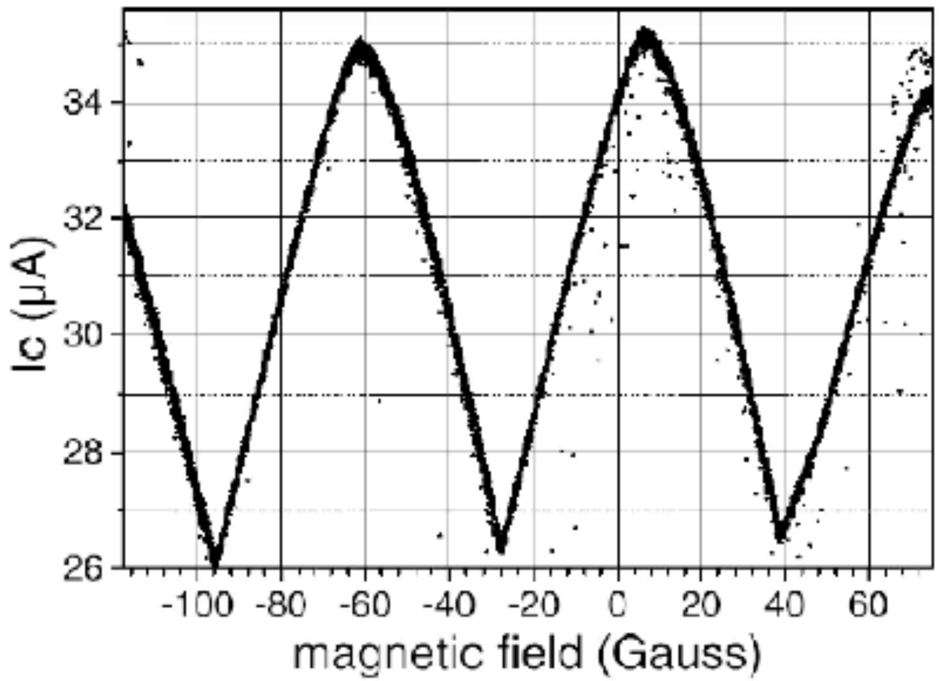

Line-width down to 10 nm.

V. Bouchiat et al, Appl. Phys. Lett. 79, 123 (2001)

Chapter 5
Nanomanipulation

5.3: Playing with molecules

Logical gates at the atomic scale

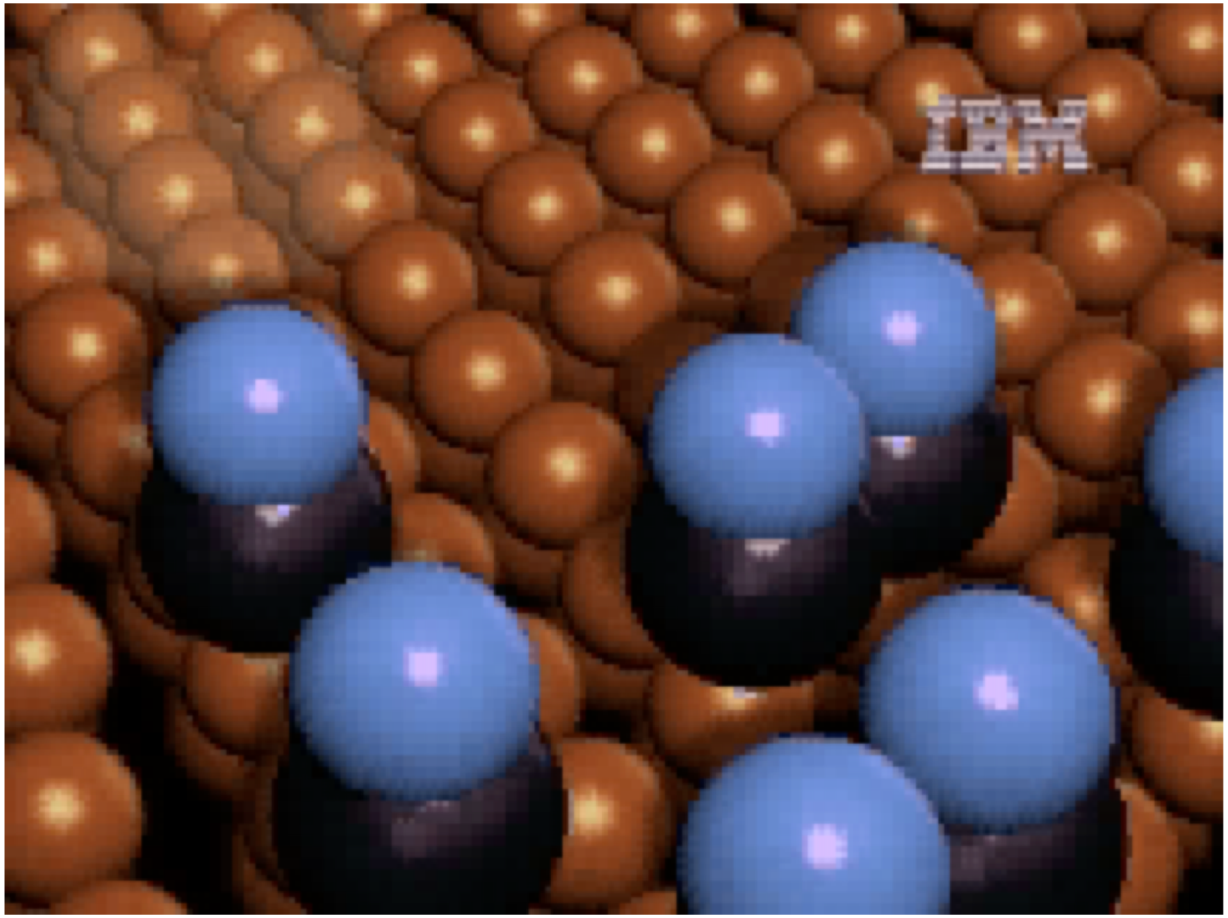

CO molecules on a Cu (111) surface.

A single move takes a few minutes at 6 K.

A. J. Heinrich, C. P. Lutz, J. A. Gupta, D. M. Eigler, Science 298, 1381 (2002).

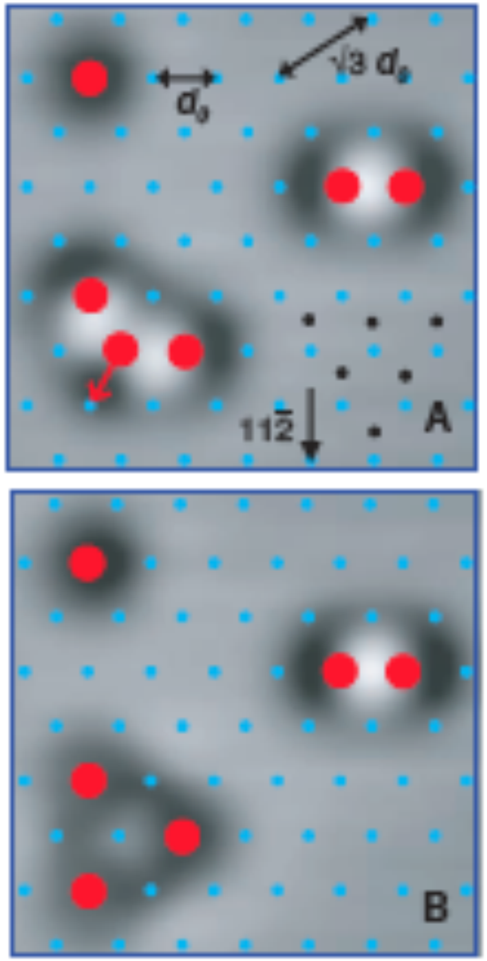

Fig. 1. STM images (1.9 nm by 1.9 nm) of CO molecules on a Cu(111) surface (I = 1 nA; V = 10 mV). The gray-scale images represent the curvature of the tip height, so local peaks appear light and local dips appear dark. Solid red circles indicate locations of CO molecules. Blue dots indicate surface-layer Cu atoms, and black dots indicate second-layer Cu atoms. d_0 is the Cu-Cu distance, 0.255 nm. (A) An isolated CO molecule (top left), a dimer (right), and a trimer in the chevron configuration (bottom left). The arrow indicates how the central CO molecule in the chevron will hop spontaneously, typically within a few minutes at 5 K. (B) The same area after the CO molecule has hopped.

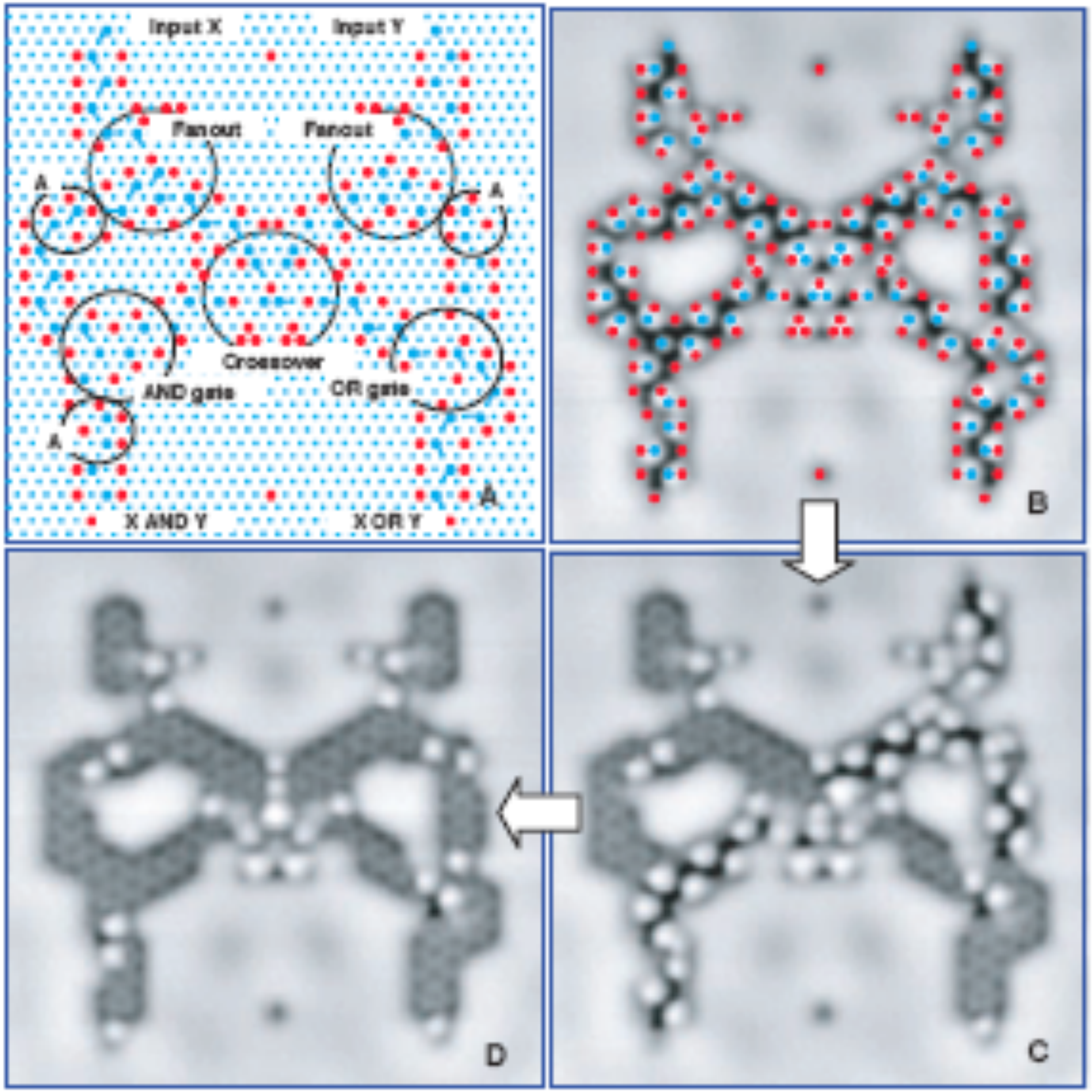

Fig. 8. Two-input sorter. (A) Model of the sorter, which computes the logic AND and logic OR of the two inputs. Color scheme is as in Fig. 7. Blue bars indicate hops that occurred when input X was triggered. The sorter consists of several components interconnected by linked-chevron cascades. (B to D) Succession of STM images (9 nm by 9 nm) (I = 50 pA; V = 10 mV). Starting from the initial setup (B), input X was triggered by manually moving the top CO molecule, which propagated a cascade to the OR output (C). Input Y was subsequently triggered, which propagated a cascade to the AND output, as shown in (D). The sorter also operated correctly when input Y was triggered first (not shown).

Chemical reaction induced by STM

Moving molecules than can afterwards react one with the other:

Reaction at the single molecule level.

H.J. Lee, W. Ho, Science 286, 1719 (1999).

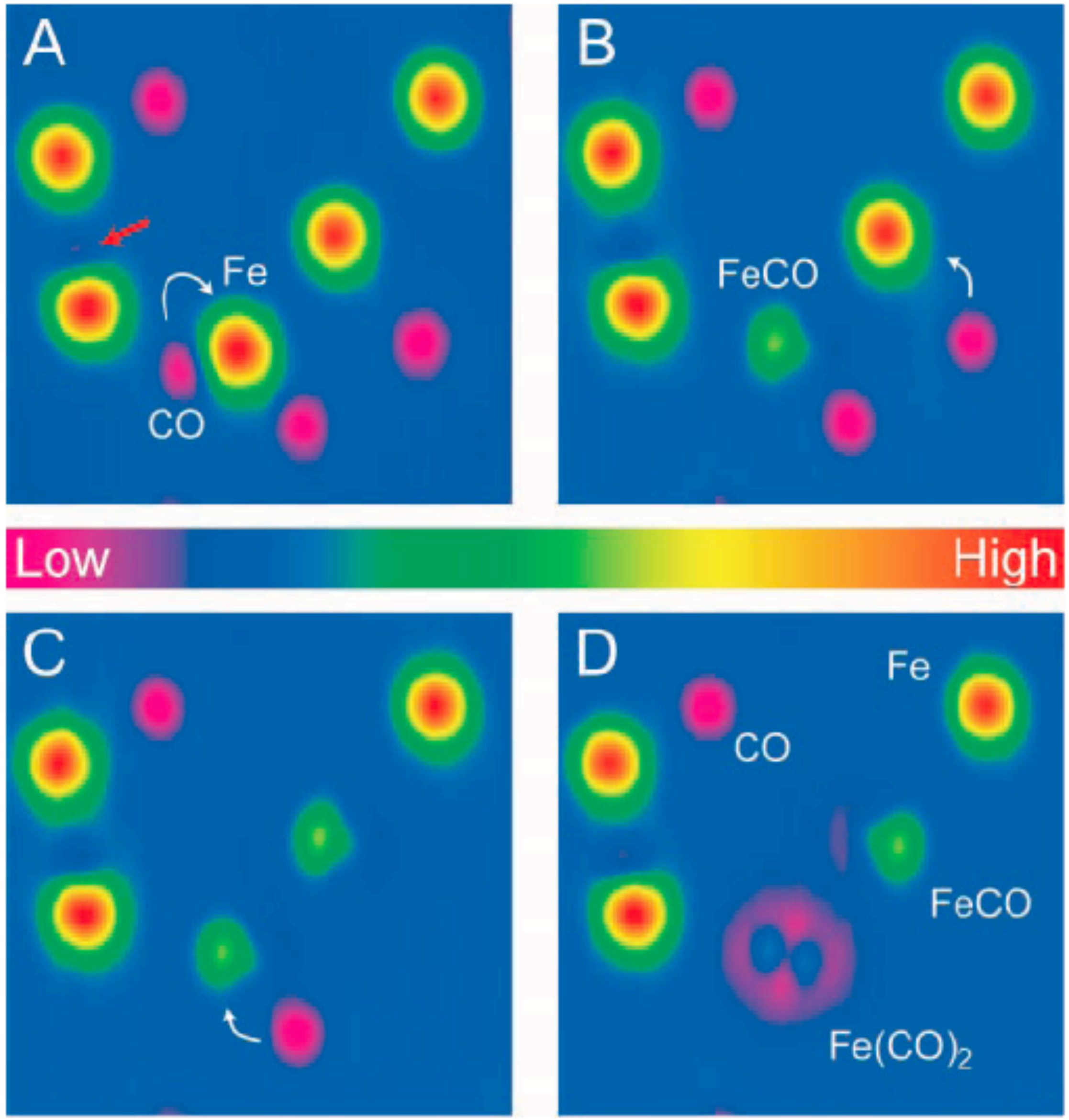

Fig. 2. A sequence of STM topographical images recorded at 70-mV bias, 0.1-nA tunneling current, and 13 K to show the formation of Fe–CO bond with the prescribed method (Fig. 1). The size of each image is 63 Å by 63 Å. Fe atoms image as protrusions and CO molecules as depressions. The white arrows indicate the pair of adsorbed species involved in each bond formation step. (**A**) Five Fe atoms and five CO molecules are adsorbed in this area of the Ag(110) surface. One CO is very close to an Fe atom (indicated by the red arrow). (**B**) A CO molecule has been manipulated and bonded to an Fe atom to form Fe(CO). (**C**) Another Fe(CO) is formed by binding CO to a second Fe atom. (**D**) An additional CO has been bonded to Fe(CO) to form $Fe(CO)_2$. A 180° flip is observed for the remaining Fe(CO).

Chapter 6
New local probes

Chapter 6
New local probes

6.1: µ-SQUID microscopy

The scanning micro-SQUID microscope

An AFM microscope with a μ-SQUID Si chip used as a tip.

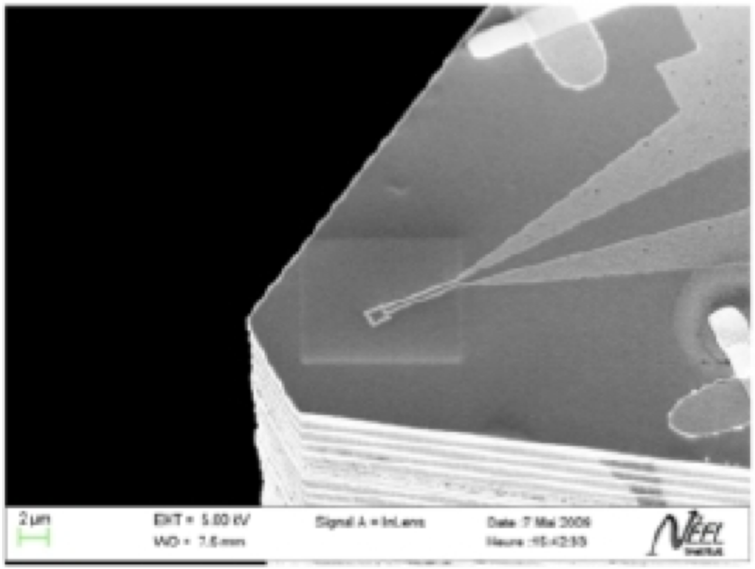

Nb μ-SQUID at the apex of a Si wafer

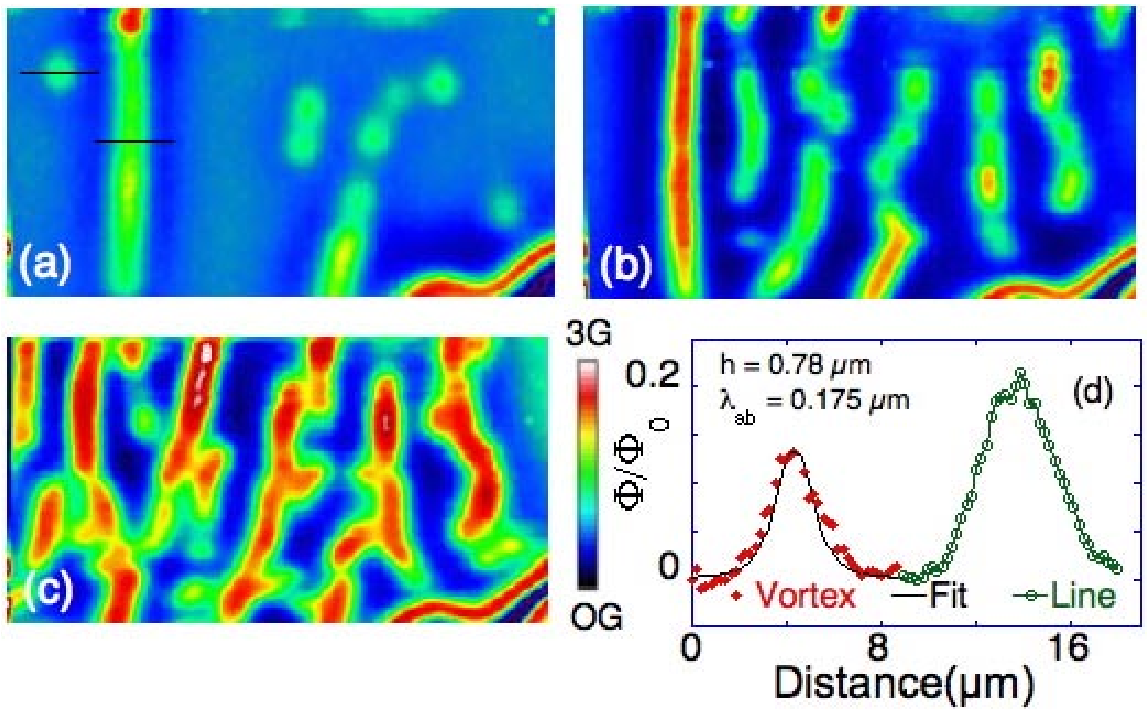

FIG. 4 (color online). Magnetic images of the flux structures in Sr_2RuO_4 at $T = 0.38$ K with magnetic field H kept constant at 10 G and tilted from c axis with an angle θ (a) 70°, (b) 60°, (c) 50°. The flux density scale is shown on the right of (c). Panel (d) shows a line plot along the line drawn in panel (a).

Magnetic imaging,

Spatial resolution of 100 nm (SQUID-sample distance).

C. Veauvy, D. Mailly and K. Hasselbach, Rev. Sci. Instrum. 73, 3825 (2002);

V. O. Dolocan, K. Hasselbach et al, Phys. Rev. Lett. 95, 097004 (2005).

Chapter 6
New local probes

6.2: Combined AFM-STM

Very low temperature AFM-STM

Need for spectroscopy of nano-circuits patterned on an insulating substrate

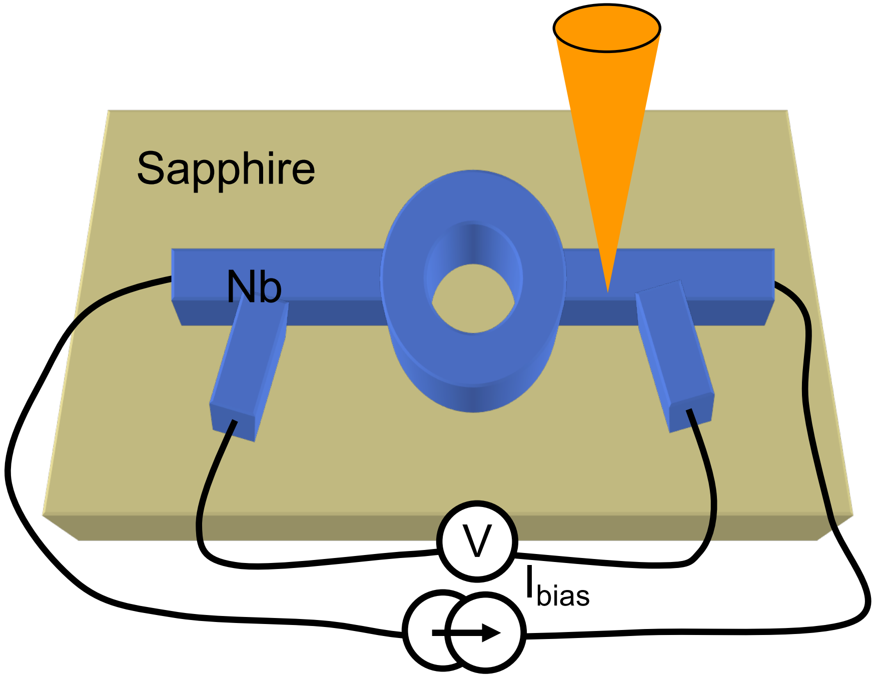

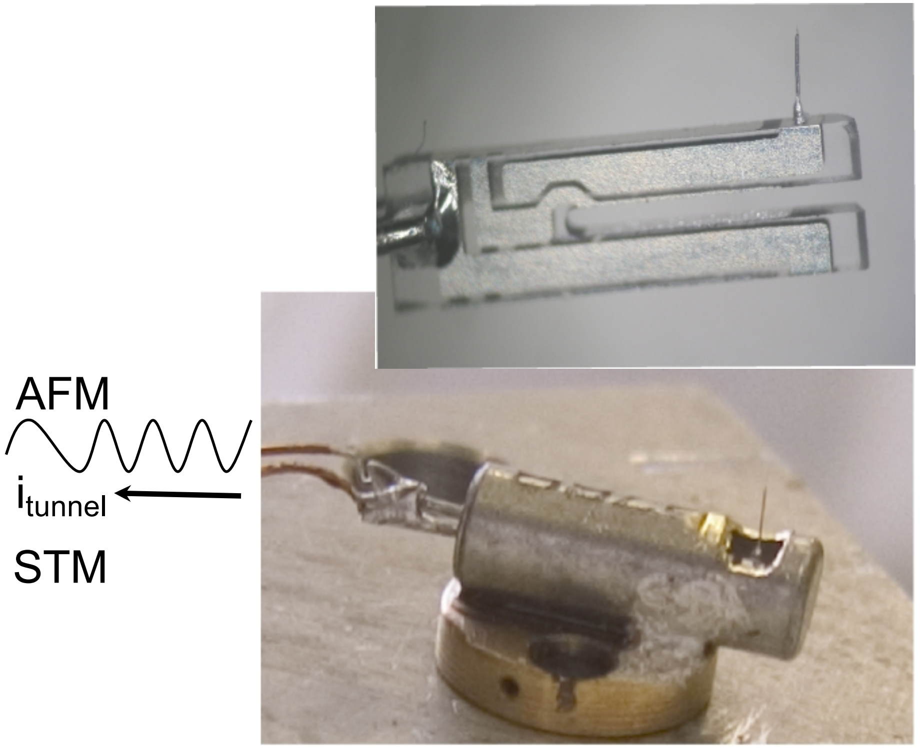

Tuning fork
+ tunnel tip (W) :
No dissipation,
Excellent stability
Excitation = pm
Oscillation = nm

1- Localization of the metallic structure with AFM

2- STM contact and spectroscopy

Non-contact, frequency modulation AFM

Interaction with the surface shifts the resonance frequency :

$$\omega = \sqrt{\frac{k_{eff}}{m}}$$

with $$k_{eff} = k_0 - \frac{\partial F}{\partial z}$$

Constant Δf = constant height

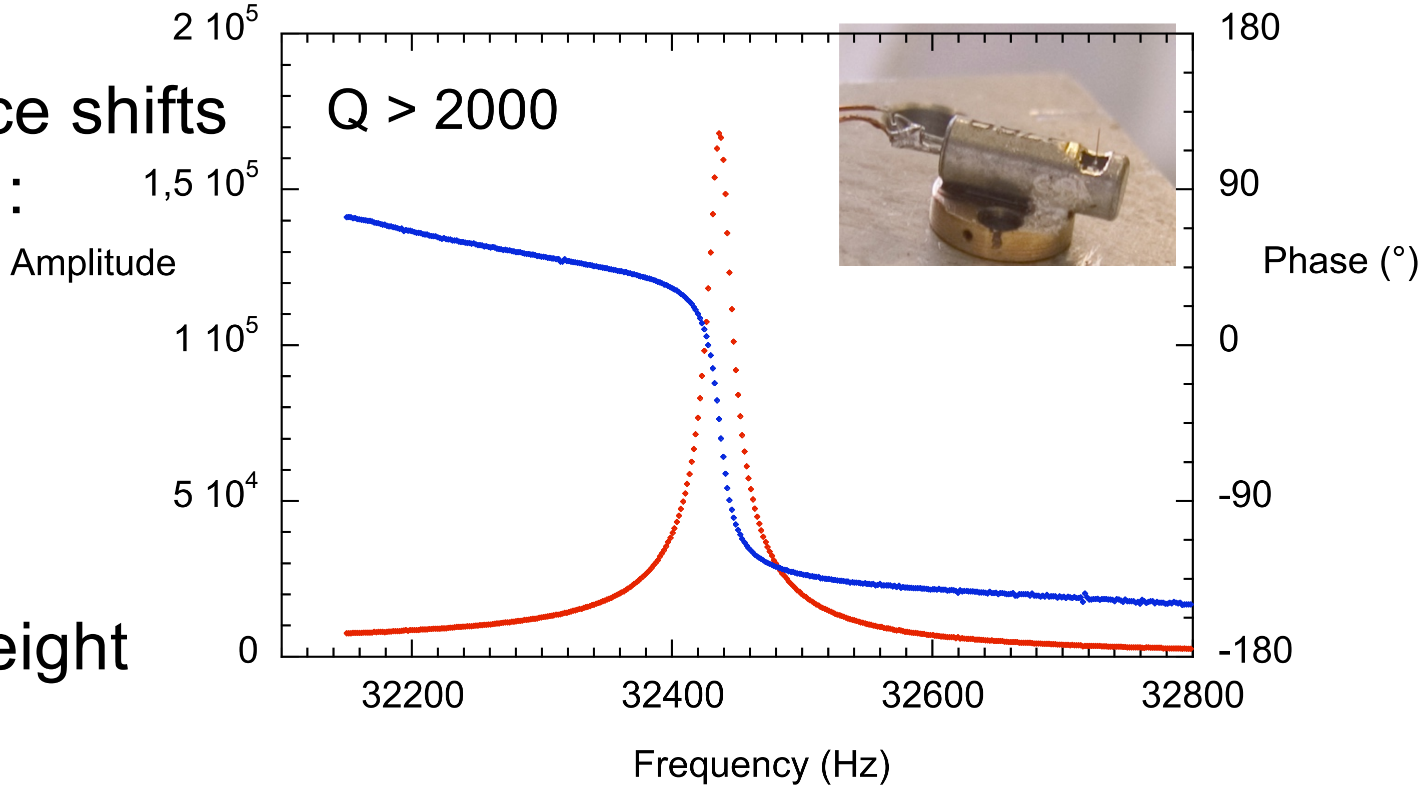

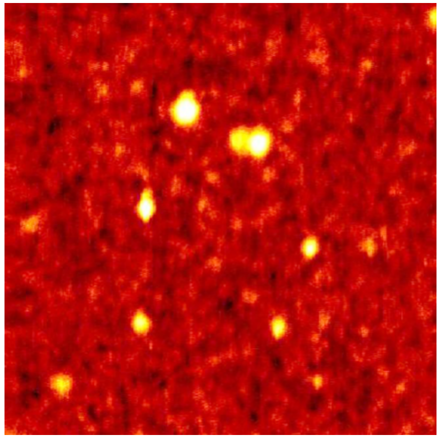

1 x 1 µm² image of 5 nm Au spheres :

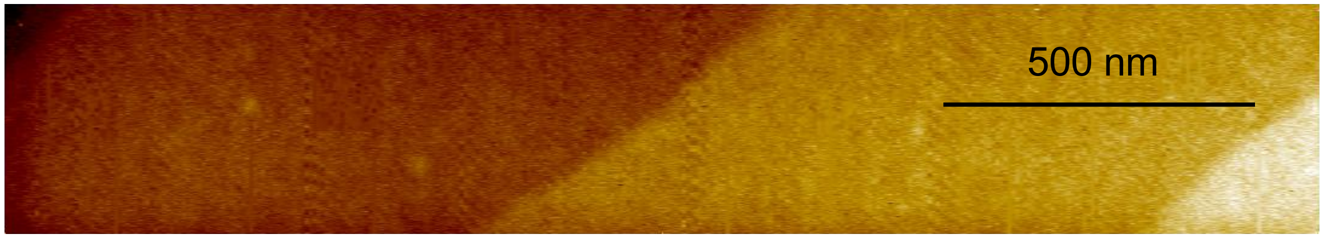

Atomic steps (0.35 nm) on sapphire :

AFM-STM at very low temperature

1: Image the nano-circuit in AFM mode

2: Probe locally the LDOS in STM mode

J. Senzier, P.S. Luo, H. Courtois, Appl. Phys. Lett. 90, 043114 (2007).

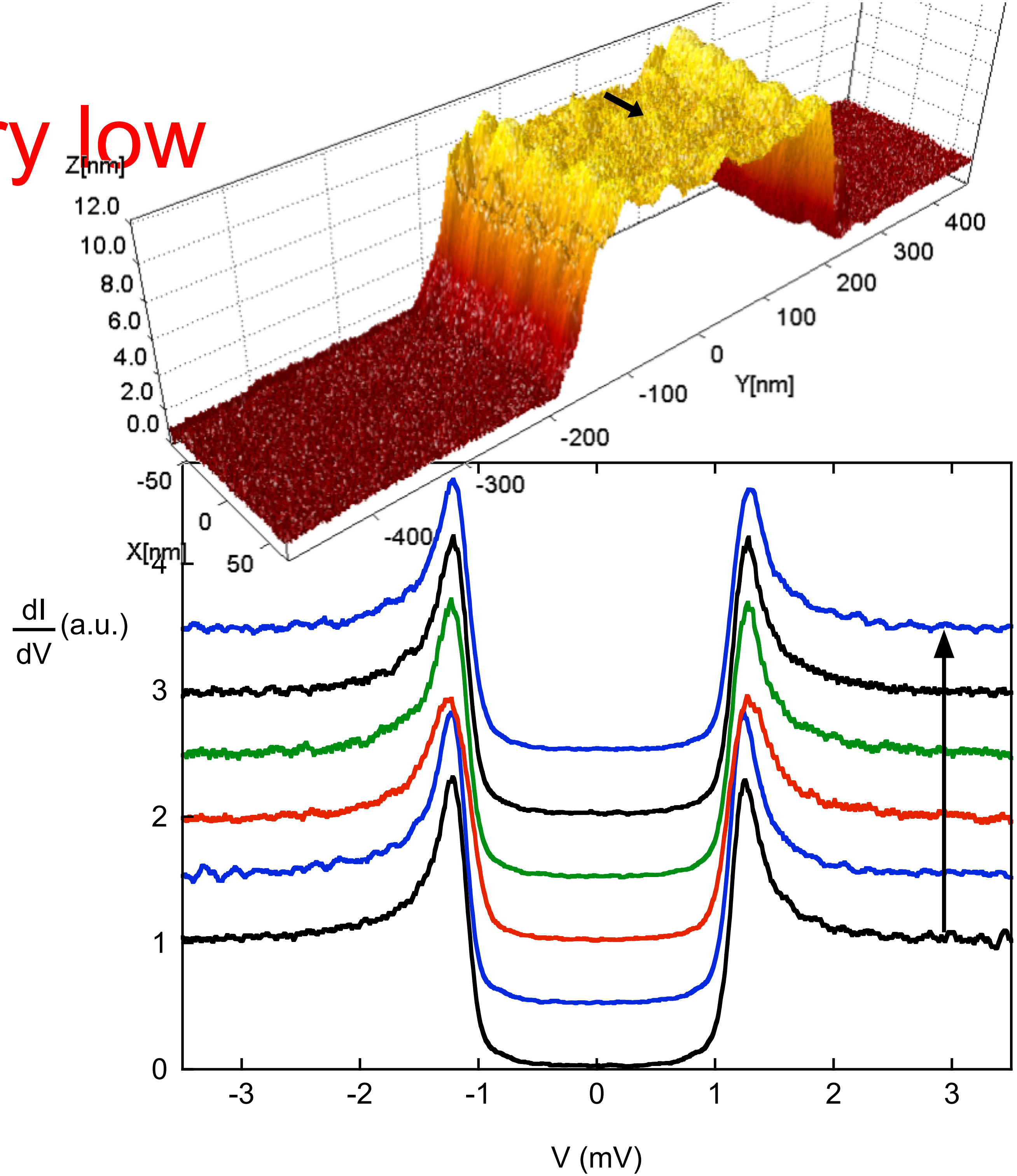

Charge disorder in a graphene device: transport properties

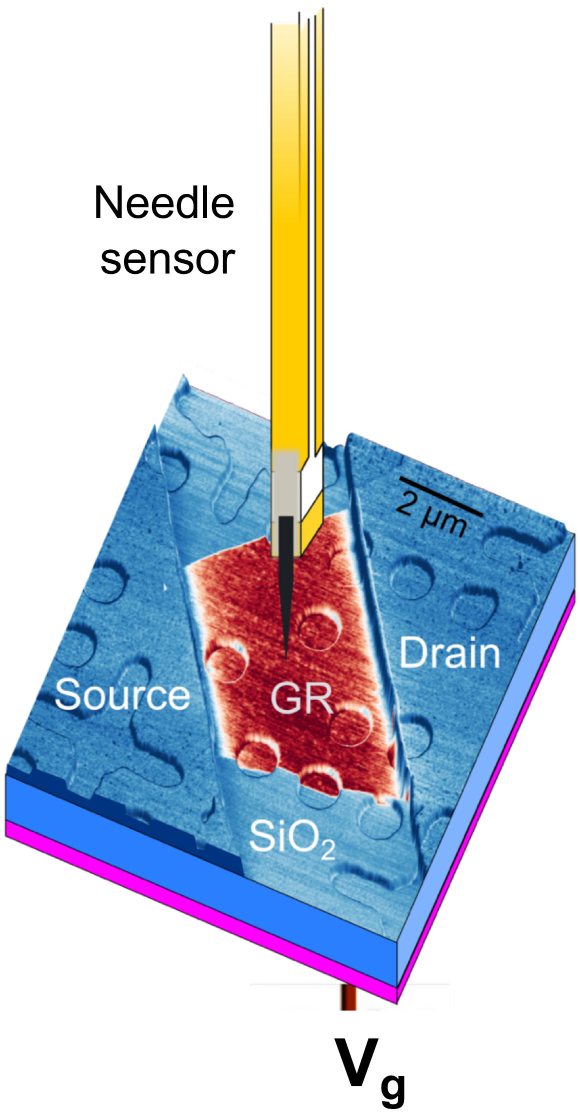

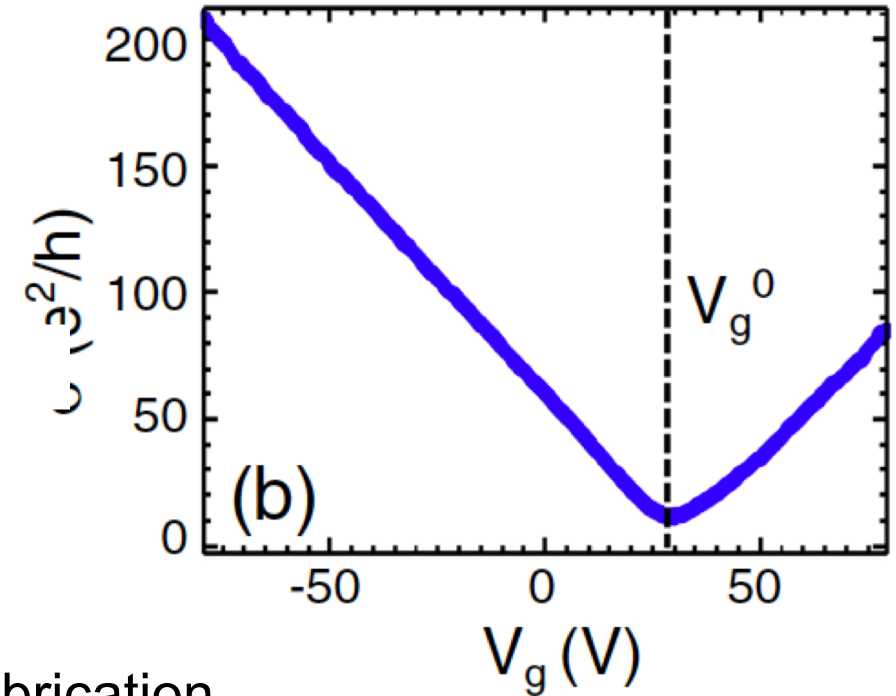

- Resist-free microfabrication
- Transport properties

mobility:	$\mu = 6000\ cm^2V^{-1}s^{-1}$
residual charge carrier density:	$n^* = 5.10^{11}\ cm^{-2}$
substrate charge impurity density:	$n_i = 8.10^{11}\ cm^{-2}$
graphene-impurity distance:	$d \approx 0.5$ nm

Puddle maps at variable charge carrier density

- dI/dV maps as a function of V_g.
- Marked maximum of puddles' size and amplitude.
- Overall charge neutrality at $V_g^D = 38$ V $\neq$ $V_g^0 = 29$ V due to gating by the tip.

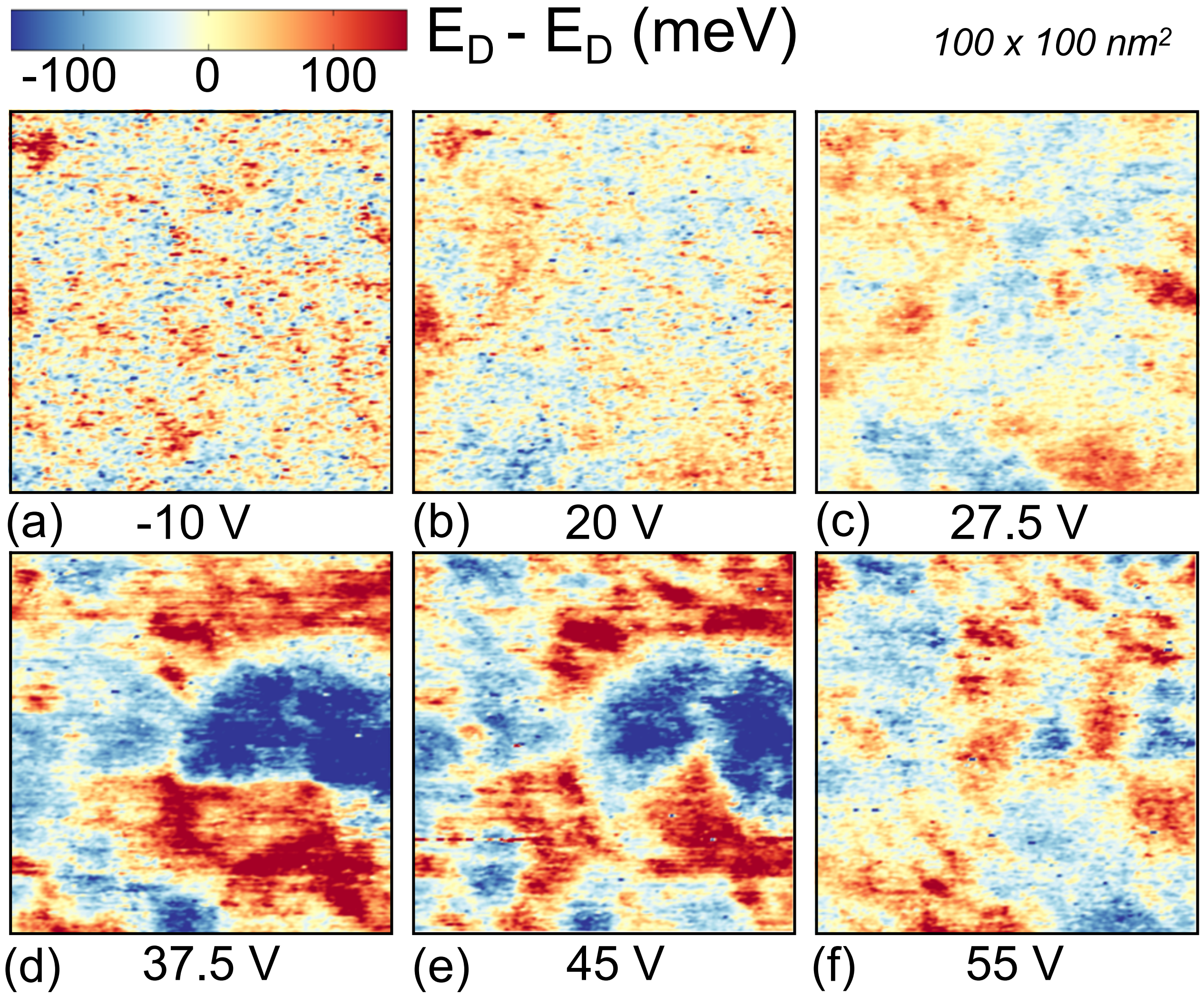

S. Samaddar, I. Yudhistira, S. Adam, H. Courtois, C.B. Winkelmann. Phys. Rev. Lett. **116**, 126804 (2016).

Conclusion

Tunnel effect is a quantum effect,

Atomic scale imaging and local spectroscopy, often mixed,

SPM instrumentation,

Nano-manipulation at different scales,

New local probes: the list is not complete.